

Eley–Rideal reaction of O^+ with oxidized Si(100)

C. L. Quinteros, T. Tzvetkov, and D. C. Jacobs^{a)}

Department of Chemistry and Biochemistry, University of Notre Dame, Notre Dame, Indiana 46556

(Received 26 June 2000; accepted 31 July 2000)

The reaction of 10–60 eV O^+ ions with a silicon oxide thin film produces scattered O_2^- . Isotopic labeling experiments demonstrate that the O_2^- product is formed by an abstraction reaction and not by physical sputtering. Energy and angle resolved detection reveals a correlation between the scattered and incident particle momenta, indicative of a direct process in which the incoming oxygen atom reacts with an adsorbed oxygen atom through an Eley–Rideal mechanism. © 2000 American Institute of Physics. [S0021-9606(00)70737-9]

Over the last few decades, extensive research efforts have uncovered many fundamental processes at the gas/surface interface.^{1–3} Scattering experiments have been instrumental in elucidating how an incident particle's energy and approach geometry affect its probability of reaction with a surface target.⁴ At thermal energies (<1 eV), molecules frequently scatter, trap, or chemisorb on a surface. In the hyperthermal energy regime (10^0 – 10^2 eV), chemical barriers are easily surmounted, and dissociative scattering, atom abstraction, and charge transfer are often observed.^{3,5,6} At collision energies above 10^2 eV, processes such as implantation and sputtering dominate.

Reactions at surfaces are often categorized as occurring through one of two mechanisms: Langmuir–Hinshelwood (LH) or Eley–Rideal (ER).⁷ In the LH mechanism, both reactant species are trapped on the surface and become thermally accommodated before they react to form a product. In the ER mechanism, an incident gaseous particle reacts directly with a surface adsorbate. In the past few years, many intermediate mechanisms have been proposed that fall in between these two extrema.⁸ Hot atom precursors are trapped but not thermally accommodated before they react, e.g., hydrogen abstraction on various surfaces.^{9–12} In a scattering-mediated ER mechanism,¹³ an incident atom undergoes a single collision with the substrate, abstracting a neighboring adsorbate on the outbound trajectory.

Most ER reactions have been studied using molecular beam techniques, where incident energies are limited to a few electron volts.^{1,14,15} Consequently, the majority of ER reactions that have been studied to date are exothermic. Many oxide surfaces are considered nonreactive because of the large binding energy of oxygen with the surface. Nevertheless, hyperthermal energy ions possess sufficient kinetic energy to activate an endothermic ER reaction. Maazouz *et al.* reported that hyperthermal energy NO^+ ions abstract oxygen atoms from O/Al(111) via an ER mechanism; this occurs in spite of the 6.8 eV endothermicity.¹⁶

The interaction of hyperthermal energy O^+ with a SiO_x surface is relevant to the low-earth orbit environment, where

energetic oxygen atoms and ions continuously bombard protective coatings, e.g., SiO_2 on orbiting spacecraft.¹⁷ Furthermore, oxygen plasma processing in the microelectronics industry is frequently used to etch and to deposit oxide films on silicon.^{18,19} Despite these important technological applications, a fundamental understanding of the reactivity of hyperthermal energy O^+ with silicon oxide is lacking. Experimental evidence is presented here to show that 16–60 eV O^+ ions directly abstract atomic oxygen from SiO_x via an ER mechanism, to form scattered O_2^- .

The experimental apparatus comprises three differentially pumped chambers. In the source chamber, a Colutron ion source produces O^+ (~96% 4S ground state) in a CO_2 plasma.²⁰ The ions are extracted, focused, and accelerated to 1300 eV before being mass selected through a Wein filter. A small aperture separates the source and buffer chambers. Deflection optics within the buffer chamber remove any neutralized hyperthermal particles. A second aperture serves as an entrance to the main chamber, wherein the ions are decelerated to 10–60 eV before striking the surface. The main chamber pressure remains at 6×10^{-10} Torr while the O^+ ion beam delivers current densities of 40–120 nA/cm².

Scattered ionic products are mass and energy analyzed with a rotatable, differentially pumped detector that includes a cylindrical electrostatic analyzer, a quadrupole mass spectrometer, and a pair of microchannel plates for single-particle detection. A *p*-doped Si(100) surface ($R=0.01$ – $0.02 \Omega \text{ cm}$) was cleaned by chemical oxidation followed by buffered HF dipping to produce a hydrogen-terminated Si surface.²¹ The sample was introduced into the main chamber through a load-lock. Annealing to 900 °C produced a clean, well-ordered (2×1) structure as revealed by low energy electron diffraction. Thin silicon oxide films were grown on the Si(100) surface with 15–60 eV O^+ beams at 45° incidence relative to the surface normal. Todorov and Fossom have reported that 40–200 eV O^+ ions incident on Si(100) produce a 40-Å-thick oxide film;²² the film thickness saturates when the rate of oxygen deposition equals the rate of etching/sputtering. Chung and co-workers found that the electron energy loss spectroscopy spectra of a silicon oxide film, grown with 300 eV O^+ ions (dose: 3×10^{15} ions/cm²) on Si(100), resembled that of a thermally grown silicon oxide layer.^{23,24}

During O^+ ion deposition, both positively and nega-

^{a)}Author to whom correspondence should be addressed; electronic mail: Jacobs.2@nd.edu

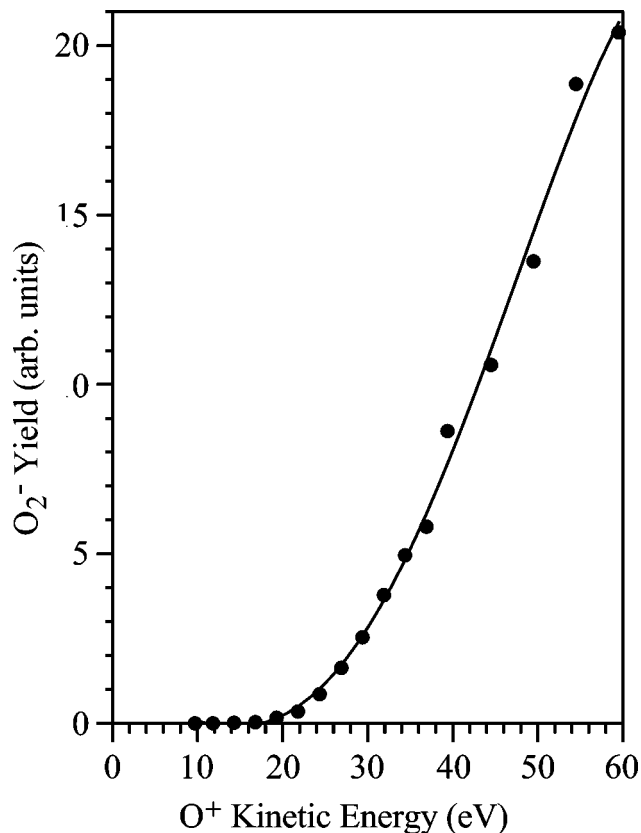


FIG. 1. O_2^- yield as a function of O^+ collision energy. O^+ is incident at 45° on an oxidized Si(100) surface. The appearance threshold for O_2^- is 16 ± 1 eV. The curve is drawn to guide the eye.

tively charged scattered products (Si^+ , SiO^+ , O^- , and O_2^-) are detected. The intensity of the O_2^- signal is an order of magnitude lower than the measured O^- signal. Scattered O^+ is not observed, indicating efficient neutralization along the inbound trajectory.²⁵ Neutralization of $O^+(^4S)$ exclusively forms $O(^3P)$, since a transition to the $O(^1D)$ or $O(^1S)$ state is spin forbidden for a one-electron transfer.

The yield of scattered O^- and O_2^- increases with O^+ dose, as the oxide film develops. After a dose of 1×10^{16} O^+ ions/cm², both anion yields reach a steady-state value. Thereafter, the composition of the outermost layers of the oxide film does not appear to change with increasing O^+ exposure. Notwithstanding, prior studies suggest that the underlying layers of the film continue to be oxidized by the incident O^+ beam until the film reaches its saturation thickness after a dose of 3×10^{17} ions/cm².²³ Only scattering results collected at 300 K in the steady-state regime (dose $> 1 \times 10^{16}$) are presented here. Figure 1 shows the O_2^- yield versus O^+ kinetic energy. The threshold for O_2^- emergence occurs at 16 ± 1 eV.

Isotopic labeling experiments help to define the origin of each oxygen atom in the O_2^- product. An isotopically pure $Si^{16}O_x$ film was grown using a mass-selected $^{16}O^+$ beam. After a $^{16}O^+$ dose of 1×10^{16} ions/cm², scattering commenced with a mass-selected $^{18}O^+$ beam. Figure 2 shows the kinetic energy distribution of scattered O_2^- for each isotopic combination. For all $^{18}O^+$ incident energies (up to 60 eV) and scattering angles studied (45° – 135°), $>98\%$ of the scat-

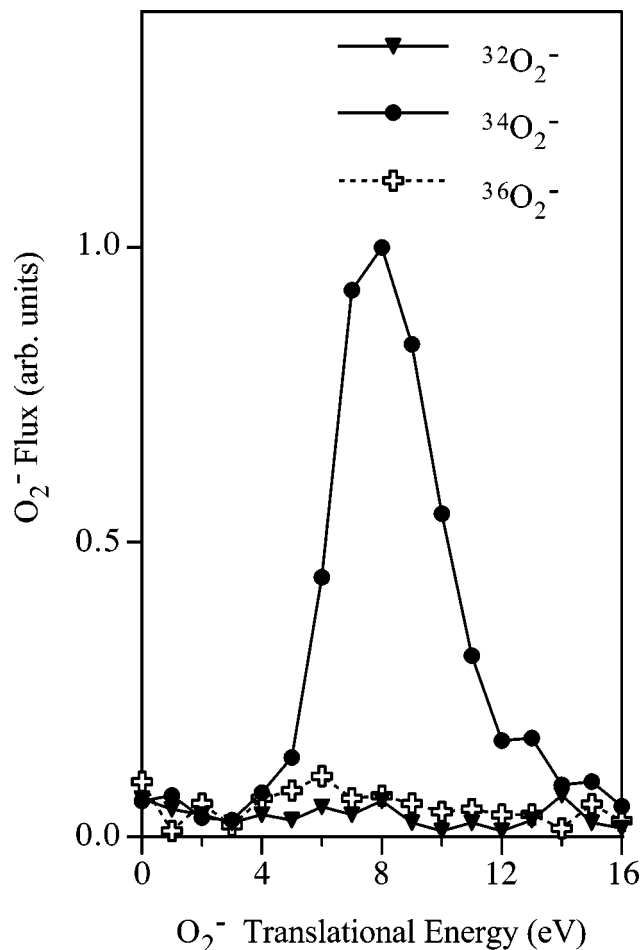


FIG. 2. Translational energy distributions of O_2^- produced from 30 eV $^{18}O^+$ incident at 45° on a $Si^{16}O_x$ thin film. Signal was collected at a 90° scattering angle for the three conceivable O_2^- masses (32, 34, and 36 u). Note that the mass 32 and 36 spectra constitute less than 2% of the total O_2^- signal.

tered O_2^- appeared at a mass equal to 34 u. Therefore, O_2^- is produced when one oxygen atom from the incident ion beam (^{18}O) combines with one oxygen atom from the silicon oxide layer (^{16}O). The lack of signal corresponding to $^{32}O_2^-$ and $^{36}O_2^-$ precludes physical sputtering and projectile recombination, respectively, as possible mechanisms for O_2^- formation. Further evidence to discard physical sputtering as a viable mechanism for O_2^- production is the observation that no appreciable O_2^- signal appears when 70 eV Ne^+ bombards the SiO_x surface.

A variety of mechanisms can describe the association of a projectile and a surface oxygen atom to form O_2^- , yet most can be eliminated in consideration of the experimental evidence. In a LH mechanism, an incoming oxygen atom would trap on the surface, become thermally accommodated, diffuse to a neighboring adsorbed oxygen atom, react, and desorb as O_2^- . The O_2^- product would then be expected to emerge with a translational energy distribution in thermal equilibrium with the surface. As Fig. 2 demonstrates, the translational energy distribution of emerging O_2^- is extremely nonthermal. Furthermore, Fig. 3 shows that the mean kinetic energy of scattered O_2^- correlates strongly with the incident O^+ kinetic energy. Therefore, the projectile (^{18}O)

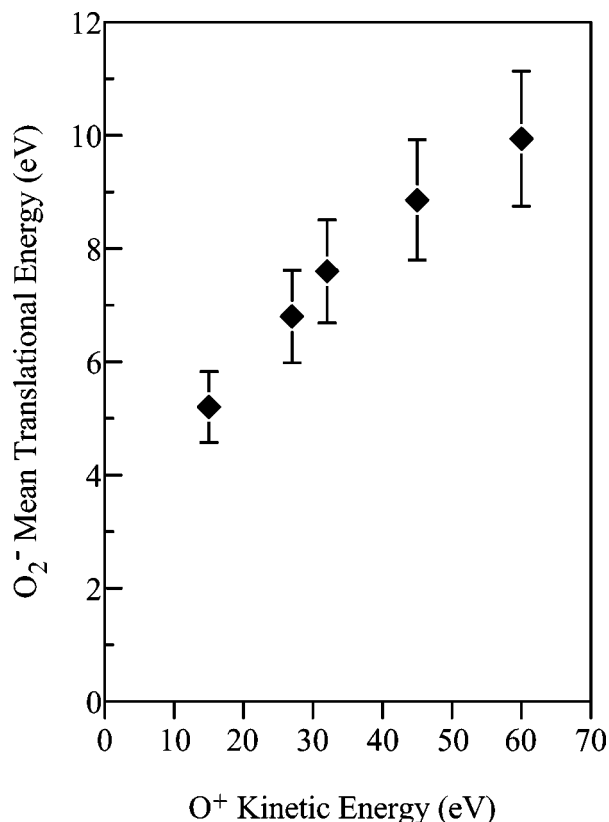


FIG. 3. Mean translational energy of scattered O_2^- product vs O^+ kinetic energy. O^+ is incident at 45° on an oxidized Si(100) surface. The mean energies are derived from a weighted average over all in-plane scattering angles.

must be reacting before it has a chance to thermally accommodate with the surface, eliminating a LH mechanism.

An alternative two-step mechanism is collision induced desorption of adsorbed oxygen, followed by gas-phase association of the sputtered oxygen anion with a scattered oxygen atom. A similar mechanism has been proposed for the production of $Cs(X)^+$ clusters ($X=Si, SiO, OH_2, OH$) in the scattering of Cs^+ on water-covered silicon.²⁶ However, in the case of O_2^- , a gas phase association reaction would generate significant vibrational excitation in the O–O stretch. Vibrationally excited O_2^- is unstable and will suffer electron autodetachment if $\nu > 3$ ($E_{vib} > 0.46$ eV) and dissociation if $E_{vib} > 4.13$ eV.²⁷ Consequently, O_2^- must be formed at the surface; in this way, the reaction's excess energy is not channeled exclusively into molecular vibration but also can be distributed into lattice excitations and product translation.

The only plausible mechanism left for O_2^- formation is an abstraction reaction. The question remains, however, as to whether the incident oxygen directly or indirectly abstracts an adsorbed oxygen atom. Examination of the product angular distribution as a function of incident angle helps to distinguish between these two cases. The angular distribution of O_2^- was measured for 45 and 60 eV O^+ ions, at incident angles of 30° and 45° . For either O^+ energy, the shape of the O_2^- angular distribution changes dramatically with incident angle. The peak of the O_2^- angular distribution shifts toward the surface normal with increasing angle of incidence. Fur-

thermore, O_2^- ions that scatter to glancing exit angles emerge with considerably more energy as the angle of incidence increases.²⁸ This strong correlation between incident and final scattering angles is consistent with a single collision event. The scattering distribution resulting from a hot-atom precursor mechanism would be uncorrelated with incident angle, because memory of the incident particle direction would be lost in the first two collisions of the hot oxygen atom with the highly corrugated surface. It is conceivable that an angular correlation could persist if the incident oxygen atom underwent a single collision with the substrate and immediately abstracted an adsorbed oxygen atom on the outgoing trajectory. Indeed, preliminary trajectory calculations confirm that it is possible for an incident oxygen atom to either directly abstract an adsorbed oxygen (ER), or to undergo a scattering-mediated ER mechanism. These simulations suggest that both pathways are capable of yielding O_2^- with less than 0.5 eV in vibrational energy, i.e., stable against electron autodetachment.

In summary, angle-, energy-, and mass-resolved detection of O_2^- emerging from the reaction of O^+ with SiO_x , implicates a direct or scattering-mediated Eley–Rideal mechanism. This study represents the first experimental evidence of hyperthermal atomic ions abstracting oxygen atoms from an oxide surface.

Support from the Air Force Office of Scientific Research (F49620-98-1-0029) is gratefully acknowledged. The authors thank M. Maazouz for insightful discussions and X. Qin for his assistance with data collection.

¹C. T. Rettner, D. J. Auerbach, J. C. Tully, and A. W. Kleyn, *J. Phys. Chem.* **100**, 13021 (1996), and references therein.

²E. W. Kuipers, A. Vardi, A. Danon, and A. Amirav, *Phys. Rev. Lett.* **66**, 116 (1991).

³J. R. Morris, G. Kim, T. L. O. Barstis, R. Mitra, C. L. Quinteros, and D. C. Jacobs, *Nucl. Instrum. Methods Phys. Res. B* **125**, 185 (1997).

⁴D. C. Jacobs, *J. Phys. C* **7**, 1023 (1995), and references therein.

⁵W. Qinyuan and L. Hanley, *J. Phys. Chem.* **97**, 2677 (1993).

⁶M. R. Morris, D. E. Riederer, Jr., B. E. Winger, R. G. Cooks, T. Ast, and C. E. D. Chidsey, *Int. J. Mass Spectrom. Ion Processes* **122**, 181 (1992).

⁷W. H. Weinberg, *Dynamics of Gas–Surface Interactions*, edited by C. T. Rettner and M. N. R. Ashfold (Royal Society of Chemistry, London, 1991), p. 171.

⁸S. Wehener and J. Kuipers, *J. Chem. Phys.* **109**, 294 (1998), and references therein.

⁹P. Kratzer, *J. Chem. Phys.* **106**, 6752 (1997).

¹⁰S. Caratzoulas, B. Jackson, and M. Persson, *J. Chem. Phys.* **107**, 6420 (1997).

¹¹A. Dinger, C. Lutterloh, and J. Kupfers, *Chem. Phys. Lett.* **311**, 202 (1999).

¹²J. Y. Kim and J. Lee, *Phys. Rev. Lett.* **82**, 1325 (1999).

¹³S. I. Yi and W. H. Weinberg, *Surf. Sci.* **415**, 274 (1998).

¹⁴C. R. Arumainayagam and R. J. Madix, *Prog. Surf. Sci.* **38**, 1 (1991).

¹⁵J. R. Engstrom, D. J. Bonser, and T. Engel, *Surf. Sci.* **268**, 238 (1992).

¹⁶M. Maazouz, T. L. O. Barstis, P. L. Maazouz, and D. C. Jacobs, *Phys. Rev. Lett.* **84**, 1331 (2000).

¹⁷E. Murad, *Annu. Rev. Phys. Chem.* **49**, 73 (1998).

¹⁸S. C. Mcnevin, *J. Vac. Sci. Technol. B* **8**, 1185 (1990).

¹⁹N. Herbots, O. C. Hellman, P. Ye, X. Wang, and O. Vancauwenberghe, *Low Energy Ion–Surface Interactions*, edited by J. W. Rabalais (Wiley, New York, 1994), Chap. 8.

²⁰B. M. Huges and T. O. Tiernan, *J. Chem. Phys.* **55**, 3419 (1971).

²¹P. Dumas, Y. J. Chabal, and P. Jakob, *Surf. Sci.* **270**, 867 (1992).

²²S. S. Todorov and E. R. Fosum, *Appl. Phys. Lett.* **52**, 48 (1988).

- ²³J. W. Chung, D. H. Baek, B. O. Kim, H. W. Yeom, and C. Y. Kim, *Phys. Rev. B* **45**, 1705 (1992).
- ²⁴D. H. Baek, B. O. Kim, J. I. Jeong, C. Y. Kim, and J. W. Chung, *J. Appl. Phys.* **69**, 3354 (1991).
- ²⁵J. S. Martin, J. N. Greeley, J. R. Morris, B. T. Feranchak, and D. C. Jacobs, *J. Chem. Phys.* **100**, 6791 (1994).
- ²⁶M. C. Yang, C. H. Hwang, and H. Kang, *J. Chem. Phys.* **107**, 2611 (1997).
- ²⁷J. H. Rechten, U. Imke, K. J. Snowdon, P. H. F. Reijnen, P. J. Vandenhoeck, A. W. Kleyn, and A. Namiki, *Nucl. Instrum. Methods Phys. Res. B* **48**, 339 (1990).
- ²⁸C. L. Quinteros, T. Tzvetkov, and D. C. Jacobs (unpublished).